PERGAMON

Computers & Geosciences 29 (2003) 787–794

COMPUTERS & GEOSCIENCES

www.elsevier.com/locate/cageo

Pecube: a new finite-element code to solve the 3D heat transport equation including the effects of a time-varying, finite amplitude surface topography☆

Jean Braun*

Research School of Earth Sciences, The Australian National University, Canberra, ACT 0200, Australia

Received 24 September 2001; received in revised form 30 September 2002; accepted 22 October 2002

Abstract

A robust finite-element code (**Pecube**) has been developed to solve the three-dimensional heat transport equation in a crustal/lithospheric block undergoing uplift and surface erosion, and characterized by an evolving, finite-amplitude surface topography. The time derivative of the temperature field is approximated by a second-order accurate, mid-point, implicit scheme that takes into account the changing geometry of the problem. The method is based on a mixed Eulerian–Lagrangian approach that requires frequent re-interpolation of the temperature field in the vertical direction to ensure accuracy. From the computed crustal thermal structure, the temperature history of rock particles that, following an imposed tectonic scenario, are exhumed at the Earth's surface, is derived. These $T-t$ paths can then be used to compute apparent isotopic ages for a range of geochronometers. The usefulness of the code is demonstrated by computing the predicted distribution of (U–Th)/He apatite ages in a high relief area of the Sierra Nevada, California, for a range of tectonic scenarios and comparing them to existing data.

Keywords: Heat transfer equation; Numerical modelling; Time-varying surface topography; Low-T geochronology; Relief evolution

1. Introduction

Much effort has recently been devoted to understanding the coupling between tectonics and erosion (Beaumont et al., 1999). Determining the rate at which landforms adapt to a changing tectonic environment has become an important problem to address. To achieve this, new low-temperature thermochronometric techniques have been developed such as (U–Th)/He apatite thermochronometry (Zeitler et al., 1987; Farley et al., 1996; Wolf et al., 1996). To interpret age data from systems characterized by closure temperatures as low as 65°C, one must thus understand how surface topography affects the thermal structure of the uppermost crust. Much work has already been devoted to this problem (Turcotte and Schubert, 1982; Stüwe et al., 1994; Mancktelow and Grasemann, 1997), but only the case of a "static" surface topography has been considered so far. To derive information on the rate of change of surface topography from thermochronometric data requires us, however, to better understand and quantify the effect of an evolving surface topography on the shape of the underlying isotherms.

Here, a new finite-element code is presented to solve the heat transfer equation in a crustal block undergoing uplift and denudation, and characterized by an evolving surface topography. The code has been designed for ease-of-use by non-specialists. It is available by contacting the author, or may be downloaded from the IAMG server.

☆Code available from server at http://www.iamg.org/CGEditor/index.htm

*Tel.: +61-2-6125-5512; fax: +61-2-6125-5443.

E-mail address: jean.braun@anu.edu.au (J. Braun).

0098-3004/03/$ - see front matter
doi:10.1016/S0098-3004(03)00052-9

2. Differential and finite-element equation

In order to study the effect of an evolving topography on the temperature field in the underlying crust/lithosphere, one must solve the following transient, three-dimensional heat transfer equation, which may be written as (Carslaw and Jaeger, 1959)

$$\rho c\left(\frac{\partial T}{\partial t}+v\frac{\partial T}{\partial z}\right)=\frac{\partial}{\partial x}k\frac{\partial T}{\partial x}+\frac{\partial}{\partial y}k\frac{\partial T}{\partial y}+\frac{\partial}{\partial z}k\frac{\partial T}{\partial z}+\rho A, \tag{1}$$

where $T(x,y,z,t)$ is the temperature, ρ is rock density, c is heat capacity, v is the vertical velocity of rocks with respect to the base of the crust/lithosphere ($z=-L$), k is conductivity and A is radioactive heat production. This equation must be solved for a given initial temperature distribution

$$T_0 = T_0(x,y,z,t=0) \tag{2}$$

and a set of boundary conditions

$$T(x,y,z=-L,t)=T_1, \tag{3}$$

$$T(x,y,z=S(x,y,t),t)=T_{MSL}+\beta S, \tag{4}$$

$$\frac{\partial T}{\partial n}=0 \quad \text{along the side boundaries}, \tag{5}$$

where $S(x,y,t)$ is the assumed, time-varying geometry of the surface of the earth, T_1 is the assumed temperature at the base of the model (the Moho or the base of the lithosphere, for example), T_{MSL} is the temperature at a reference surface elevation (mean sea level, for example), and β is the lapse rate, i.e. the rate of change of temperature with elevation in the earth's atmosphere. n is the outward normal to the side boundaries.

An analytical solution to the steady-state form of this equation ($\partial T/\partial t=0$ and $S(x,y,t)=S(x,y,t=0)$) exists (Stüwe et al., 1994). The transient solution requires, however, the use of numerical methods. The approach presented here is based on the finite-element method (Zienkiewicz, 1977), using six- or eight-node prismatic finite elements, built on the assumption that, within each element, the temperature varies linearly in all directions. The finite-element equation corresponding to the heat transfer equation is (Bathe, 1982)

$$M\frac{\partial T}{\partial t}+(K_a+K_c)T=M\dot{T}+KT=F, \tag{6}$$

where

$$M=\int_V H^T\rho c H\,\mathrm{d}V, \tag{7}$$

$$K_a=\int_V H^{*T}\rho c v B\,\mathrm{d}V, \tag{8}$$

$$K_c=\int_V B^T k B\,\mathrm{d}V, \tag{9}$$

$$F=\int_V H^T A\,\mathrm{d}V, \tag{10}$$

where V is the volume of the finite element, T is the vector of the nodal temperatures, H is the vector of the shape functions, $H_i(x,y,z)$, defining how the temperature $T(x,y,z)$ varies within each element as a function of the temperature at the nodes, T_i:

$$T(x,y,z)=\sum_{i=1}^{6/8} H_i(x,y,z)T_i \tag{11}$$

and B is the matrix describing the spatial derivatives of the temperature:

$$B=\begin{bmatrix}\frac{\partial H_i}{\partial x}\\ \frac{\partial H_i}{\partial y}\\ \frac{\partial H_i}{\partial z}\end{bmatrix}. \tag{12}$$

To improve stability in situation's where heat advection dominates over diffusion, a streamline-upwind Petrov–Galerkin method is used (Hughes and Brooks, 1982) and

$$H^*=H+\tau v B_3, \tag{13}$$

where

$$\tau=\frac{\Delta z\sqrt{15}}{|v|} \tag{14}$$

and Δz is a vertical lengthscale (the thickness of the element).

To account for the time-varying geometry of the upper surface, a Lagrangian approach is used which consists in vertically translating the top nodes of the mesh, i.e. those located along the top surface, by the required amount, $\dot{S}(x,y,t)\Delta t$, at the start of each time step. Note that this translation is independent of the velocity v which represents the Eularian velocity of rocks with respect to the base of the model (at $z=-L$). In cases where $\dot{S}<v$, erosion takes place; in cases where $\dot{S}>v$, deposition (sedimentation) takes place. This method is accurate providing $\Delta t<\Delta z/10|\dot{S}|$, where $|\dot{S}|$ is the rate of change of the surface topography. The vertical translation of nodes may lead to mesh distortion and an inaccurate solution to the equation. To circumvent this problem, the temperature field is interpolated from the deformed mesh onto an "undeformed" mesh at the end of each time step. This procedure is illustrated in Fig. 1.

To ensure numerical stability, a second-order accurate, mid-point, implicit scheme ($\alpha=0.5$) is used to represent the time derivative of temperature

(Belytschko et al., 1979):

$$\frac{T(t+\Delta t)-T(t)}{\Delta t}=\dot{T}(t+\Delta t)\alpha+\dot{T}(t)(1-\alpha). \tag{15}$$

The finite-element equations are rewritten, taking into account that the geometry of the problem (i.e. the surface) may be changing from one time step to the next

$$(M(t+\Delta t)+\alpha\Delta t K(t+\Delta t))\ T(t+\Delta t) \tag{16}$$

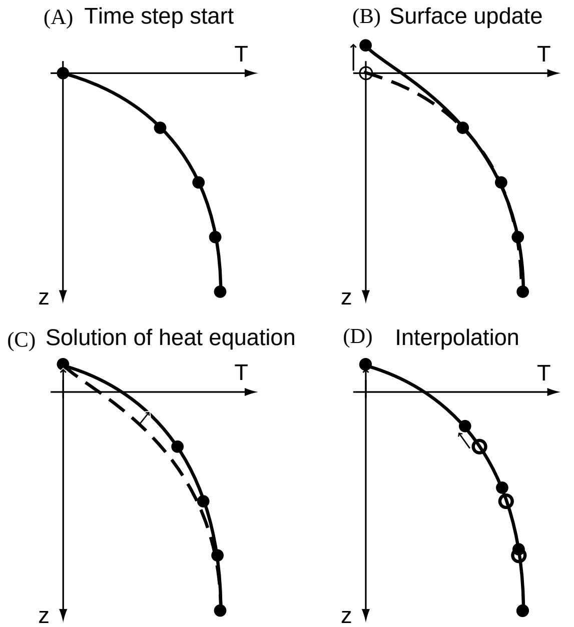

Fig. 1. Illustration of Lagrangian method. (A and B) Effect of vertical movement of upper boundary; (C) Eq. (1) is solved over time step Δt; and (D) interpolation from "deformed" grid, represented by open circles, onto "undeformed", original grid represented by dark circles.

$$\begin{aligned}&=(M(t+\Delta t)-(1-\alpha)\Delta t K(t))\ T(t)\\&\quad+\ \Delta t(\alpha F(t+\Delta t)+(1-\alpha)F(t)).\end{aligned} \tag{17}$$

Note that it is assumed that

$$M(t)M^{-1}(t+\Delta t)\approx I. \tag{18}$$

The large system of algebraic equations that results from the finite-element discretization of the basic heat transfer equation is solved by a Gauss–Seidel iterative method with over-relaxation (Bathe, 1982) or a conjugate gradient method with an element-by-element preconditioning (Hughes et al., 1984).

3. Comparison to analytical solution

To illustrate the accuracy of the numerical method, its predictions are compared to a semi-analytical solution (Stüwe et al., 1994) to the problem of a steadily eroding lithospheric layer of thickness $L=100$ km characterized by a finite-surface topography of wavelength $\lambda=12.5$ km and amplitude $h_0=1$ km. In Fig. 2, the geometry of the 65°C isotherm is shown for four values of the exhumation rate as derived from the numerical solution of the problem and its semi-analytical solution. The basal temperature is assumed to be 1000°C and the thermal diffusivity ($\kappa=k/\rho c$) is 25 km^2 Myr^{-1}. In all cases, the numerical solution compares very well with the semi-analytical one.

4. Pecube

Pecube has been developed as a user-friendly ForTran90 program. The user can describe the problem to solve in one of two ways (Fig. 3): through a detailed ASCII input file (*Pecube.in*) or by modifying one of the subroutines (*create_pecube_in.f90*) which will create the input file. The

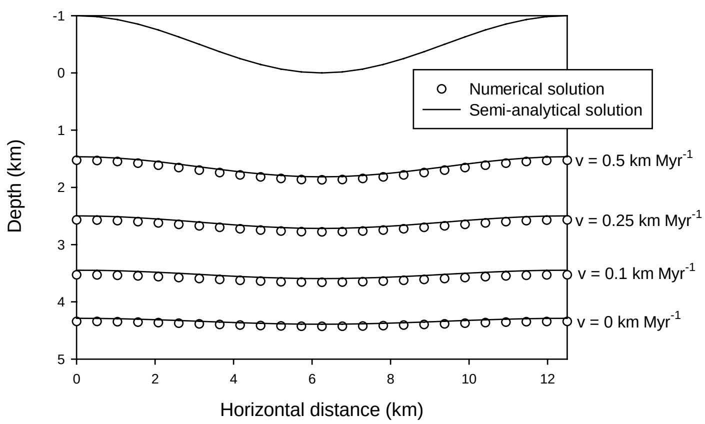

Fig. 2. Comparison between semi-analytical solution (lines) from Stüwe et al. (1994) and predictions from numerical model presented here (circles). See text for problem description and parameters.

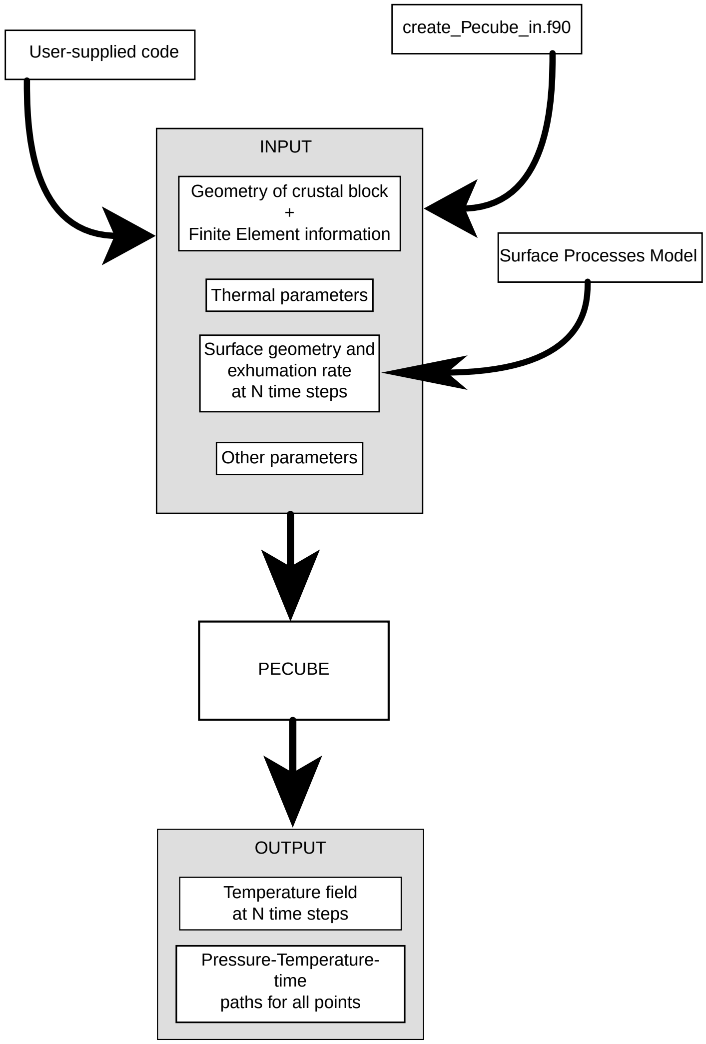

Fig. 3. Flow chart describing various input options of Pecube as well as input parameters and output fields.

format of the input file has been designed for ease-of-use by non-specialists, yet it permits to solve a large range of tectonically interesting problems. It includes basic information such as the number of nodes, their horizontal coordinates, the number and type of elements, and the connectivity matrix (relating the elements to the nodes). For ease of use, it is assumed that thermal properties such as rock conductivity, heat capacity, density and heat production are spatially uniform and constant through time. Other parameters such as crustal thickness, basal temperature, surface temperature and lapse rate must also be defined. The exhumation velocity is assumed to be spatially uniform but can change through time. The surface topography is specified by defining the height above mean sea level of each node at a series of times in the past, t_i, $i = 1, \ldots, n$. Elevation values can be produced from a DEM or derived from the output of a surface processes model (SPM), such as *Cascade* (Braun and Sambridge, 1997). This is the reason why triangular and rectangular prismatic elements are used in Pecube. The output consists of the complete three-dimensional temperature structure at the times t_i as well as pressure (depth) and temperature values experienced through time by rocks that end up at the surface of the model at t_n. These P–T–t paths can be used to predict rock ages for any thermochronometric system or metamorphic assemblages. A detailed user guide is supplied with the software.

Note that the time step, Δt, is determined internally to ensure accuracy for any set of input parameters according to

$$\Delta t = \min\left(\frac{\rho c L^2}{100k}, \frac{\Delta z}{2|v|}, \frac{\Delta z_S}{10|\dot{S}|}\right), \tag{19}$$

where Δz is the height of the smallest element and Δz_S is the height of the smallest element in contact with the surface.

5. Example: thermal structure beneath Kings Canyon

To illustrate the usefulness of Pecube, it was applied to studying the time evolution of the thermal structure beneath the surface topography of the Kings Canyon area in the Sierra Nevada, California, which has recently been documented by (U–Th)/He apatite thermochronometry (House et al., 1998). Several hypotheses exist on the origin of the present-day relief (House et al., 1998). The potential contributing factors are: rapid uplift and erosion during the Laramide Orogeny, some 90–100 Myr ago, and a more recent (late Tertiary) episode of relief rejuvenation following local uplift and/or climate change.

Results based on two end-member tectonic/geomorphic scenarios are presented. Both assume that, at the end of the Laramide Orogeny, surface relief was approximately twice as large as today's. In the first scenario, relief amplitude decays rapidly after the Laramide Orogeny (i.e. within 20 Myr) to one-tenth of its present-day value and is rejuvenated in the last 5 Myr, whereas, in the second scenario, relief amplitude decays steadily over the last 90 Myr.

In both cases, it is assumed that the temperature is fixed at 500°C at the base of the crust ($z = 35$ km) and at 15° along the top surface (the lapse rate is neglected), that exhumation rate was high (1 km Myr^{-1}) during the Laramide Orogeny (between 110 and 90 Myr ago) and very low (0.03 km Myr^{-1}) between 90 Myr ago and the present. Heat diffusivity ($k/\rho c$) is set at 25 km^2 Myr^{-1}, and heat production is neglected. The problem is solved on a $51 \times 51 \times 35$ mesh with a spatial resolution of 1 km in all directions. The geometry of the surface topography is extracted from a 1-km-resolution DEM (GTOPO30). Changes in relief are incorporated by modifying the amplitude of the topography, not its shape. This implies that the geometry of the drainage system (i.e. the location of the major river valleys) has not changed in the last 110 Myr. Detailed analysis of (U–Th)/He ages across Kings Canyon and adjacent deeply incised valleys indicates that this is a good assumption (House et al., 1998, 2001).

The results are shown in Fig. 4 as three-dimensional perspective plots of the finite-element mesh on the sides of which contours of the temperature field have been superimposed. Three critical times are shown: at the end the Laramide Orogeny and, for each experiment, 20 Myr later and at the end of computations (i.e. present day). The contours of temperature clearly show the effect of vertical heat advection, especially at the end of the orogenic phase (Fig. 4A), where the isotherms are compressed towards the surface and deformed by the high relief surface topography. After 20 Myr, the two scenarios diverge greatly. The system has almost reached conductive equilibrium beneath a flat surface under scenario 1 (Fig. 4B), while, under scenario 2, the low-temperature isotherms are deformed by the presence of a high relief topography (Fig. 4C). The predicted present-day temperature structures are relatively similar in both scenarios. In the first case (Fig. 4D), the isotherms are perturbed by the finite-amplitude surface topography, whereas, in the second case (Fig. 4E), the topography is too young to affect the underlying thermal structure.

6. Application of the method to thermochronometry

As stated earlier, Pecube predicts $T - t$ paths for all rock particles which, at the end of computations, occupy the location of the nodes along the top surface of the finite-element mesh. From these $T - t$ paths, an apparent (U–Th)/He age for apatite can be computed at each location, following the procedure and parameter values given by Wolf et al. (1998) and Farley (2000). Colour contours of the predicted ages have been superimposed on the surface topography of the last two panels of Fig. 4. The computed mean ages are relatively similar (60.94 and 68.71 Myr, respectively). These depend mostly on the assumed age for the end of the Laramide Orogeny. The distributions of ages on the landscape are, however, very different (compare Figs. 4D and E). Following the first scenario (Fig. 4D), most ages are comprised between 30 and 70 Myr with a very clearly defined linear relationship between age and elevation. In the second scenario (Fig. 4E), the range of predicted ages is similar (40–90 Myr) but their relationship to elevation is less clear. At the scale of a single river valley (< 10 km), ages are proportional to elevation but, at the larger scale (> 10 km), older ages are found at lower elevation, i.e. near the valleys.

Thus, while the two scenarios lead to very similar predictions for the thermal structure beneath Kings Canyon and the mean (U–Th)/He ages in apatite, they predict very different relationships between age and elevation. This is further documented in Fig. 5 where the predicted ages are plotted against surface elevation for the two scenarios. In the first scenario (grey circles), there is a clear linear relationship between age and elevation. The slope of the regression line between age and elevation is related to the exhumation rate (Stüwe et al., 1994). In the second scenario (grey squares), this relationship is not so clear and ages vary by as much as 50 Myr at any given elevation. In Fig. 5, recently published data collected in the Sierra Nevada area (House et al., 1998), across Kings Canyon and the adjacent Tuolumne, Merced and San Joaquin drainage systems, have been superimposed on the model

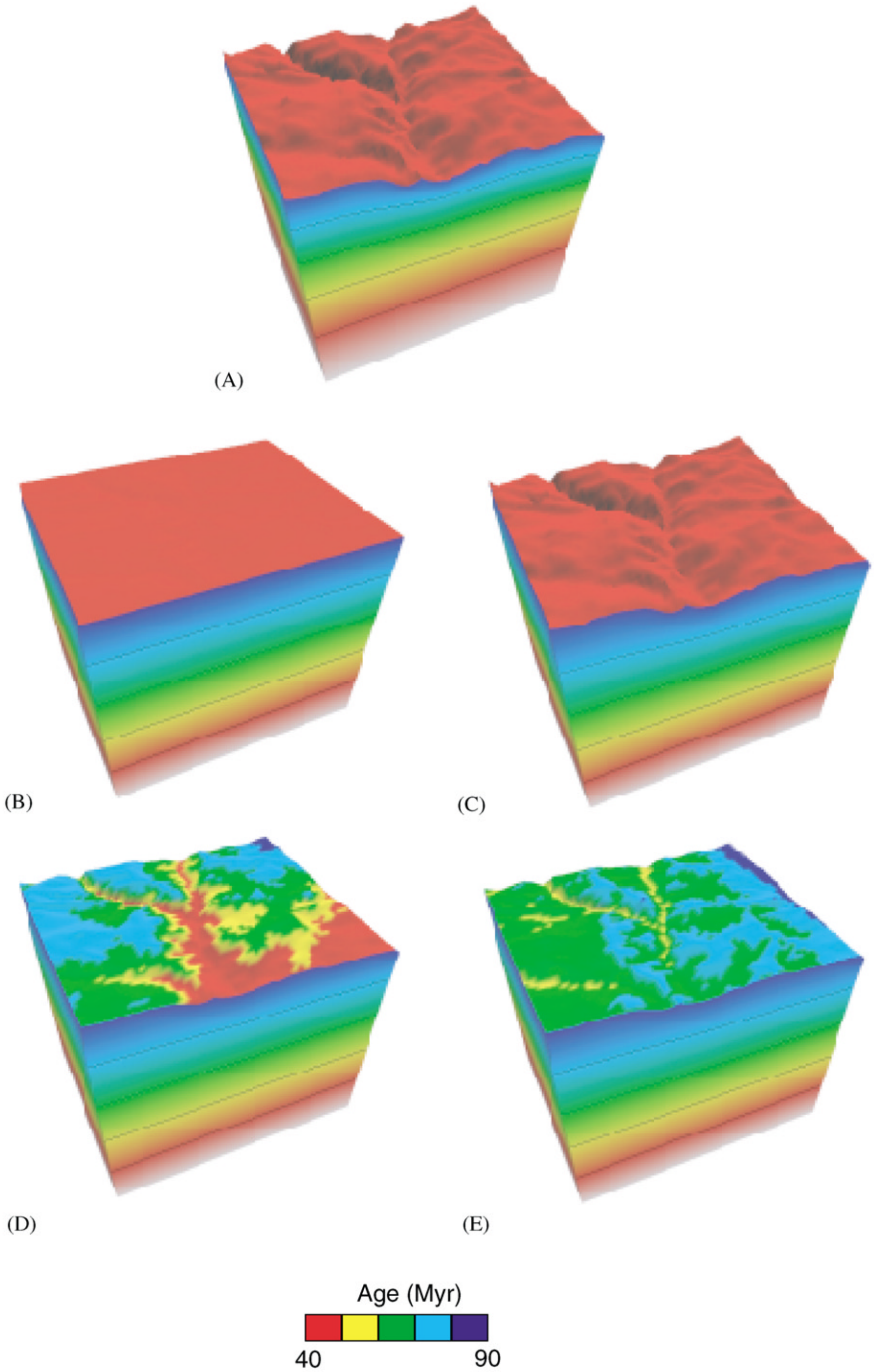

Fig. 4. Perspective view of finite-element domain with temperature field contoured on sides. (A) Solution at end of Laramide Orogeny; (B) 20 Myr later following scenario 1 and (C) scenario 2; (D) solution at end of computations (corresponding to present day) following scenario 1 and (E) scenario 2. Age contours superimposed on surface in panels (D) and (E).

predictions (black circles). The data, collected across a limited range of elevations (1.8–2.2 km) shows a pattern similar to the predictions of scenario 2 (i.e. large age variations at constant elevation). However, another dataset collected along the valley wall of Kings Canyon (House et al., 1997), across a very short distance (<2.5 km) but covering a larger range of elevations (0.5–2.2 km), shows a clear linear relationship between

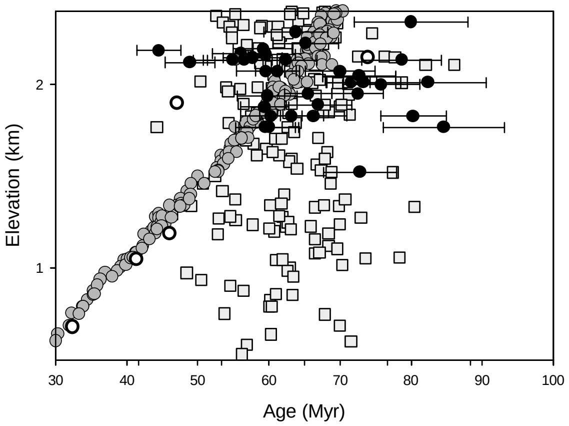

Fig. 5. Predicted and observed (U–Th)/He apatite ages against elevation. Black circles correspond to data collected across entire Sierra Nevada batholith but for limited range of elevations (House et al., 1998); white circles are ages collected along steep transect within Kings Canyon (House et al., 1997); grey circles are ages predicted following scenario 1; grey squares correspond to scenario 2.

age and elevation, much more similar to the predictions derived from scenario 1. This result, therefore, indicates that more work is necessary to understand how the relationship between rock ages and elevation is affected by sampling interval, i.e. the length scale over which ages are collected.

7. Conclusions

A new, user-friendly, finite-element code has been developed to solve the heat transport equation in three dimensions in a region of the earth's crust undergoing exhumation and characterized by a changing, finite-amplitude surface topography. The usefulness of the model, called Pecube, has been demonstrated by computing maps of predicted ages for (U–Th)/He in apatite in the Kings Canyon area (California), which have been directly compared to existing data. The predictions from two different tectonic/geomorphic scenarios clearly show that, low-temperature thermochronometers are sensitive to the evolution with time of the surface topography. In regions characterized by rapid rejuvenation of the landform in the recent past, ages increase with elevation. In regions characterized by a slowly decaying surface topography, the relationship between age and elevation is more complex, and appears to be a function of the wavelength of the topography (i.e. the width of valleys). This observation indicates that there is a need to properly understand the effect of a changing surface topography on the thermal structure in the underlying crust, to retrieve meaningful information regarding the tectonic and geomorphic evolution of high relief areas from low-temperature thermochronometers such as (U–Th)/He in apatite. Pecube is ideally suited to perform this task.

Acknowledgements

The author would like to thank L. Moresi and G. Beardsmore for very constructive reviews of this manuscript.

References

Bathe, K.-J., 1982. Finite Element Procedures in Engineering Analysis, 1st Edition. Prentice-Hall, Englewood Cliffs, NJ, 735pp.

Beaumont, C., Kooi, H., Willett, S., 1999. coupled tectonic-surface process models with applications to rifted margins and collisional orogens. In: Summerfield, M. (Ed.), Geomorphology and Global Tectonics. Wiley, New York, pp. 29–55.

Belytschko, T., Yen, H.-J., Mullen, R., 1979. Mixed methods for time integration. Computer Methods in Applied Mechanics and Engineering 17, 18, 259–275.

Braun, J., Sambridge, M., 1997. Modelling landscape evolution on geological time scales: a new method based on irregular spatial discretization. Basin Research 9, 27–52.

Carslaw, H.S., Jaeger, C.J., 1959. Conduction of Heat in Solids, 3rd Edition. Clarendon Press, Oxford, 510pp.

Farley, K.A., 2000. Helium diffusion from apatite: general behavior as illustrated by Durango fluorapatite. Journal of Geophysical Research 105 (B2), 2903–2914.

Farley, K.A., Wolf, R., Silver, L., 1996. The effect of long alpha-stopping distances on (U–Th)/He dates. Geochemica et Cosmochemica Acta 60, 4223–4229.

House, M.A., Wernicke, B.P., Farley, K.A., Dumitru, T.A., 1997. Cenozoic thermal evolution of the central Sierra Nevada, California, from (U–Th)/He thermochronometry. Earth and Planetary Science Letters 151, 167–169.

House, M.A., Wernicke, B.P., Farley, K.A., 1998. Dating topography of the Sierra Nevada, California, using apatite (U–Th)/He ages. Nature 396, 66–69.

House, M.A., Wernicke, B.P., Farley, K.A., 2001. Paleo-geomorphology of the Sierra Nevada, California, from (U–Th)/He ages in apatite. American Journal of Science 396, 66–69.

Hughes, T., Brooks, A., 1982. A theoretical framework for Petrov–Galerkin methods with discontinuous weighting functions: applications to the streamline-upwind procedure. In: Gallagher, R.H., Norrie, D.H., Oden, J.T., Zienkiewicz, O.C. (Eds.), Finite Elements in Fluids. Wiley, New York, pp. 47–65.

Hughes, T.J.R., Raefsky, A., Muller, A., 1984. A progress report on EBE solution procedures in solid mechanics. In: Taylor, C., Owen, D., Hintons, E. (Eds,), Numerical Methods for Nonlinear Problems, Vol. 2. Proceedings of the Second International Conference, Universidad Polytechnica de Barcelone, Spain, pp. 18–109.

Mancktelow, N.S., Grasemann, B., 1997. Time-dependent effects of heat advection and topography on cooling histories during erosion. Earth and Planetary Science Letters 270, 167–195.

Stüwe, K., White, L., Brown, R., 1994. The influence of eroding topography on steady-state isotherms. Application to fission track analysis. Earth and Planetary Science Letters 124, 63–74.

Turcotte, D.L., Schubert, G., 1982. Geodynamics: Applications of Continuum Physics to Geological Problems, 1st Edition. Wiley, New York, 456pp.

Wolf, R.A., Farley, K.A., Silver, L.T., 1996. Helium diffusion and low-temperature thermochronometry of apatite. Geochemica et Cosmochemica Acta 60, 4231–4240.

Wolf, R.A., Farley, K.A., Kass, D.M., 1998. Modeling of the temperature sensitivity of the apatite (U–Th)/He thermochronometer. Chemical Geology 148, 105–114.

Zeitler, P.K., Herczig, A.L., McDougall, I., Honda, M., 1987. U–Th–He dating of apatite: a potential thermochronometer. Geochemica et Cosmochemica Acta 51, 2865–2868.

Zienkiewicz, O.C., 1977. The Finite Element Method, 3rd Edition. McGraw-Hill, Maidenhead, England, 787pp.